AGU PUBLICATIONS

Geochemistry, Geophysics, Geosystems

RESEARCH ARTICLE
10.1002/2014GC005263

Special Section:
Mechanics, deformation, and hydrologic processes at subduction complexes, with emphasis on the NanTroSEIZE drilling transect

Large volume submarine ignimbrites in the Shikoku Basin: An example for explosive volcanism in the Western Pacific during the Late Miocene

Steffen Kutterolf[1], Julie C. Schindlbeck[1], Rachel P. Scudder[2], Richard W. Murray[2], Kevin T. Pickering[3], Armin Freundt[1], Shasa Labanieh[4], Ken Heydolph[1], Sanny Saito[5], Hajime Naruse[6], Michael B. Underwood[7], and Huaichun Wu[8]

[1]GEOMAR, Helmholtz Center for Ocean Research, Kiel, Germany, [2]Department of Earth and Environment, Boston University, Boston, Massachusetts, USA, [3]Department of Earth Sciences, University College London, London, UK, [4]IFREMER, Centre de Brest, Plouzane, France, [5]Institute for Research on Earth Evolution, Japan Agency for Marine-Earth Science and Technology, Yokosuka, Japan, [6]Department of Geology and Mineralogy, Kyoto, Japan, [7]Department of Geological Science, University of Missouri, Columbia, Missouri, USA, [8]School of Marine Science, China University of Geosciences, Beijing, China

Key Points:
- Two volcanic sources for Miocene Expedition 322 tuffaceous sandstones
- Large eruptions produced wide and voluminous deposits within the Shikoku Basin
- Tuffaceous sands on Philippine Plate potentially influence Nankai subduction

Supporting Information:
- ReadMe
- Tables S1–S4

Correspondence to:
S. Kutterolf,
skutterolf@geomar.de

Citation:
Kutterolf, S., J. C. Schindlbeck, R. P. Scudder, R. W. Murray, K. T. Pickering, A. Freundt, S. Labanieh, K. Heydolph, S. Saito, H. Naruse, M. B. Underwood, and H. Wu (2014), Large volume submarine ignimbrites in the Shikoku Basin: An example for explosive volcanism in the Western Pacific during the Late Miocene, *Geochem. Geophys. Geosyst.*, *15*, 1837–1851, doi:10.1002/2014GC005263.

Received 4 FEB 2014
Accepted 9 APR 2014
Accepted article online 15 APR 2014
Published online 27 MAY 2014

Abstract During IODP Expedition 322, an interval of Late Miocene (7.6 to ~9.1 Ma) tuffaceous and volcaniclastic sandstones was discovered in the Shikoku Basin (Site C0011B), Nankai region. This interval consists of bioturbated silty claystone including four 1–7 m thick interbeds of tuffaceous sandstones (TST) containing 57–82% (by volume) pyroclasts. We use major and trace element glass compositions, as well as radiogenic isotope compositions, to show that the tuffaceous sandstones beds derived from single eruptive events, and that the majority (TST 1, 2, 3a) came from different eruptions from a similar source region, which we have identified to be the Japanese mainland, 350 km away. In particular, diagnostic trace element ratios (e.g., Th/La, Sm/La, Rb/Hf, Th/Nb, and U/Th) and isotopic data indicate a marked contribution from a mantle source beneath continental crust, which is most consistent with a Japanese mainland source and likely excludes the Izu-Bonin island arc and back arc as a source region for the younger TST beds. Nevertheless, some of the chemical data measured on the oldest sandstone bed (TST 3b, Unit IIb) show affinity to or can clearly be attributed to an Izu-Bonin composition. While we cannot completely exclude the possibility that all TST beds derived from unknown and exotic Izu-Bonin source(s), the collected lines of evidence are most consistent with an origin from the paleo-Honshu arc for TST 1 through 3a. We therefore suggest the former collision zone between the Izu-Bonin arc and Honshu paleo-arc as the most likely region where the eruptive products entered the ocean, also concurrent with nearby (~200 km) possible Miocene source areas for the tuffaceous sandstones at the paleo-NE-Honshu arc. Estimating the distribution area of the tuffaceous sandstones in the Miocene between this source region and the ~350 km distant Expedition 322, using bathymetric constraints, we calculate that the sandstone beds represent minimum erupted magma volumes between ~1 and 17 km^3 (Dense Rock Equivalent (DRE)). We conclude that several large volume eruptions occurred during the Late Miocene time next to the collision zone of paleo-Honshu and Izu-Bonin arc and covered the entire Philippine Sea plate with meter thick, sheet-like pyroclastic deposits that are now subducted in the Nankai subduction zone.

1. Introduction

The Nankai Trough Seismogenic Zone Experiment (NanTroSEIZE) was initiated to observe the up-dip limit of the seismogenic zone along a subduction boundary that is well known for the occurrence of large tsunamigenic mega-thrust earthquakes [*Tobin and Kinoshita*, 2006]. The Nankai Trough, representing the surface expression of the site where the Philippine Sea plate subducts approximately normal to the strike of the trench beneath the Eurasian Plate (~4 cm/yr) [*Seno et al.*, 1993], was selected for this experiment (Figure 1). As a prerequisite for drilling to depths where earthquakes occur, several key components of the plate-boundary system needed to be investigated in order to improve our understanding of subduction inputs. Therefore, a major goal of IODP Expeditions 322 and 333 was the characterization of the presubduction inputs of sediment and oceanic basement.

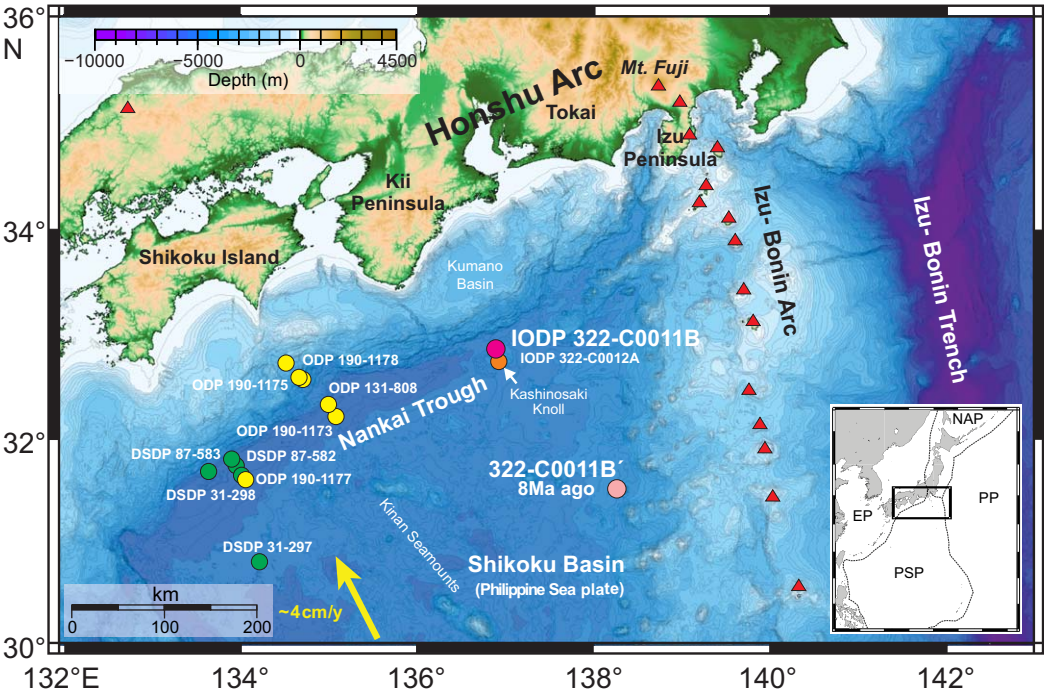

Figure 1. Bathymetric map from Nankai Trough off southwestern Japan (Yuzuru Yamamoto, personal communication, 2012). Arrow = convergence direction between Philippine Sea plate and Japan. Magenta and orange dots = Expedition 322 drilling sites, pink dot represents the location of Site C0011B at approximately 8 Ma. Previous transects of Nankai Trough (green and yellow dots) were positioned off Ashizuri and Muroto peninsulas of Shikoku. Inset shows the location of Nankai Trough: EP, Eurasian plate; PP, Pacific plate; and NAP, North American plate.

To accomplish these objectives, coring was conducted at two sites in the Shikoku Basin on the subducting Philippine Sea plate (Figure 1). IODP Sites C0011 and C0012 are located ~100 km southeast of the Kii Peninsula and ~150–200 km west of the Izu-Bonin arc at the Kashinosaki Knoll, a prominent bathymetric seafloor high. Site C0011 on the northwestern flank of the Knoll has an expanded stratigraphic section whereas Site C0012 near the crest represents a condensed sediment section above oceanic crust (Figure 1).

The Shikoku Basin, in which the subducting sediments were deposited, was created on the Philippine Sea plate during the Early and Middle Miocene by seafloor spreading in a backarc setting relative to the Izu-Bonin subduction system [*Kobayashi et al*., 1995]. The lithostratigraphy of the Shikoku Basin has historically been divided into the lower (Late to Early Miocene) and the upper (Holocene to Late Miocene) Shikoku Basin deposits [e.g., *Underwood*, 2007]. However, the lithostratigraphic results from Expedition 322 further indicate the presence of an important and additional "middle Shikoku Basin" deposit, represented by volcanogenic sandstone-rich stratigraphic Unit II (Figure 2), at least in the eastern part of the Shikoku Basin.

In total, five major stratigraphic units have been defined on the basis of lithofacies observation [*Underwood et al*., 2010] (Figure 3). Unit I (0–347.82 m bellow sea floor (mbsf)) corresponds to ash-rich, fine-grained hemipelagites with ash-layer abundance and glass-shard freshness decreasing downward [*Expedition 333 Scientists*, 2011]. An abrupt lithologic change at 347.82 mbsf marks the Unit I/Unit II boundary with the appearance of coarser-grained tuffaceous sandstones (Figures 2 and 3) and heterolithic gravel and sand in low to moderately bioturbated silty claystones. The age of Unit I ranges from Quaternary to Late Miocene (0 to ~7.6 Ma) whereas Unit II (347.82–479.06 mbsf) comprises sediments from 7.6 to ~9.56 Ma [*Zhao et al*., 2013]. Underlying Units III to V reach an age of 18.9 Ma at the basement/sediment boundary at Site C0012.

This paper uses geochemical data to constrain the source region of Unit II volcanic matter-rich beds and assess volume estimates for their related eruptive events. The question if the sandstone beds have been fed by the proximal (Izu-Bonin arc and rear arc) or more distal (Japanese mainland) source area will help to constrain the distribution of these sheet-like deposits [see *Pickering et al*., 2013] of the middle Shikoku Basin on the incoming Philippine plate and allow further research on their possible influence on the Nankai subduction zone. The mode of formation of these beds is discussed elsewhere [*Schindlbeck et al*., 2013].

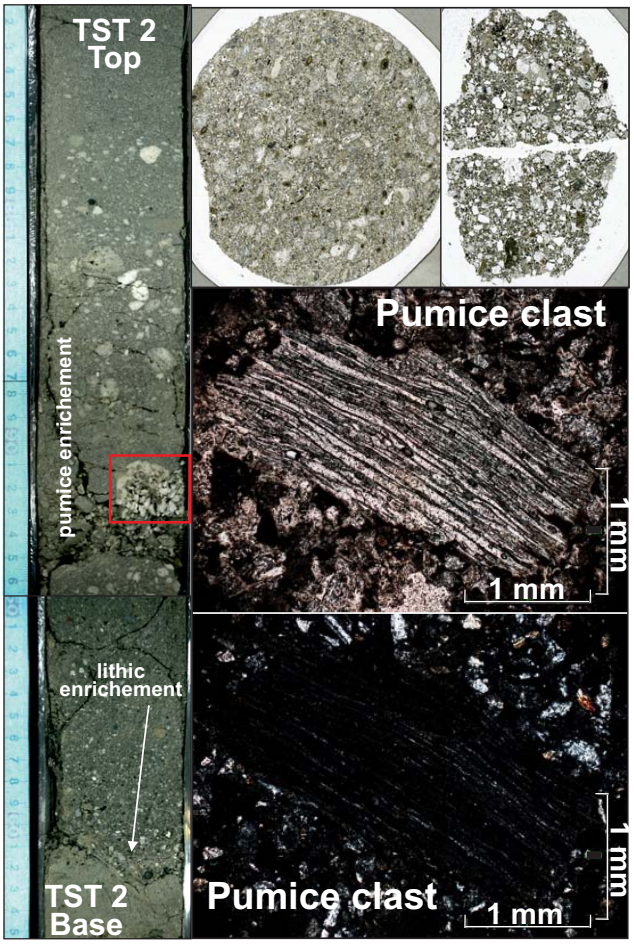

Figure 2. Top left panel: top part of tuffaceous sandstone 2 core segment from Unit IIa with pumice enrichment; bottom left panel: bottom part of tuffaceous sandstone 2 core segment from Unit IIa with lithic enrichment. Top right panel: pumice clasts in thin sections from tuffaceous sandstone two and three in whole slides. Middle right panel: pumice clast in thin section as close up in polarized light. Lower right panel: pumice clast in thin section as close in polarized light with crossed Nichols.

2. Samples and Methods

We have quantified lithologic components by point counting of 85 shipboard smear-slides of Unit II sediments [*Underwood et al.*, 2010] (Figure 4 and Table S1) and analyzed geochemical compositions of glass shards and pumice fragments of 31 sandstone samples, using electron microprobe for major elements (15–20 individual shards per sample) on all samples, and laser ablation ICP-MS for trace elements (1–16 individual shards per sample) on nine selected tuffaceous sandstone samples (Table S2).

2.1. Electron Microprobe

Glass shards analyses (465) were performed by electron microprobe (EMP) for major and minor elements as described in *Kutterolf et al.* [2011]. EMP analyses were conducted on epoxy embedded samples with a JEOL JXA 8200 wavelength dispersive electron microprobe at GEOMAR, Kiel, using 15 kV accelerating voltage, a beam defocused to 5 μm with currents of 6 nA for felsic glass, and counting times of 20–40 s for most major and minor elements and 10–20 s for backgrounds. Natural and synthetic glasses and minerals were used as standards for calibration. Accuracy has been monitored by standard measurements on Lipari obsidian while 50 individual glass shard measurements are bracketed by two standard measurements at the beginning and the end of each analytical series. Regarding 54 monitor measurements standard deviation on Lipari [e.g., *Hunt and Hill*, 2001] is $<$0.5% for silica, between 1% and 7% (Na_2O, K_2O, FeO_{tot}, CaO, Al_2O_3) and 14–19% (TiO_2, MgO) for the other major elements (except for MnO_2 and P_2O_5; see supporting information Table S4). All analyses are normalized to 100% to eliminate the effects of variable postdepositional hydration and analysis with total oxides $<$85 wt % have been excluded from the data set to avoid obvious effects of alteration throughout all elements. Finally, 393 microprobe analyses have passed the quality check since accidental shots on microcrystal have also been excluded from the data set.

2.2. LA-ICPMS

Trace element concentrations of 45 glass shards have been conducted by laser ablation inductively coupled plasma-mass spectrometry (LA-ICP-MS) at Frankfurt University (1) and GEOMAR (2) using (1) a Merchantek LUV213TM petrographic laser microprobe in conjunction with a Finnigan MAT ELEMENT2TM high-resolution ICP double-focusing mass spectrometer and a laser beam that was set to 30 μm in diameter and operated in ultra-violet modus at 213 nm using Q-switched laser energy of 2 mJ and a 5 Hz repetition rate; (2) a 193 nm excimer laser ablation system (Coherent, GeoLasPro) coupled to a double-focusing, high-resolution magnetic sector mass spectrometer (Nu Instruments, AttoM) and a laser beam that was set between

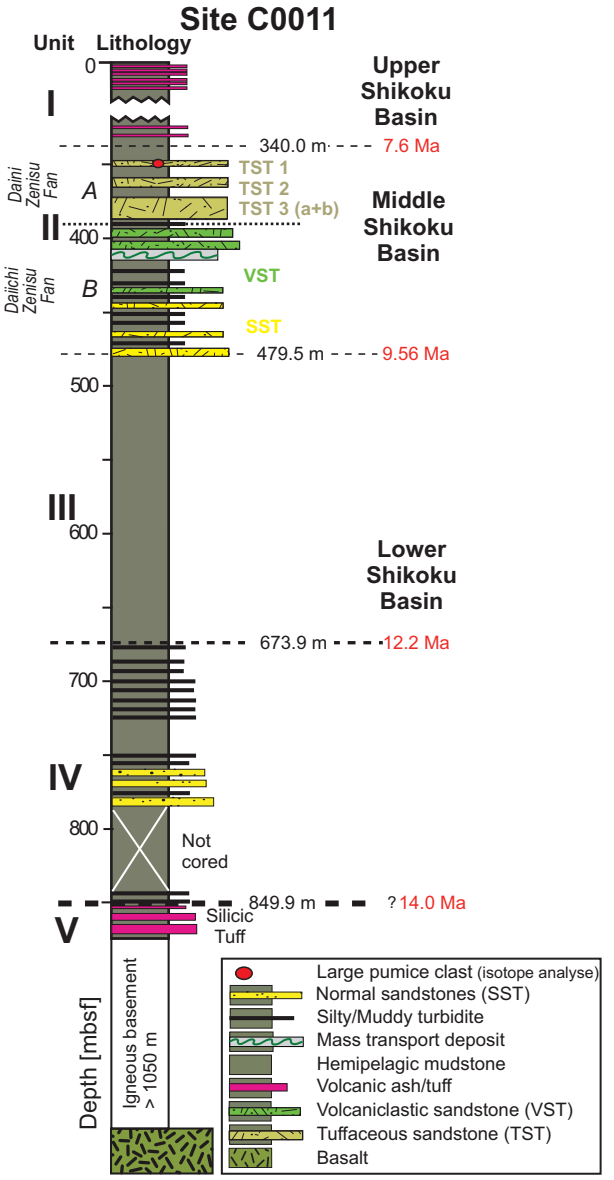

Figure 3. Stratigraphic succession of drill Site C0011 with lithologic units after *Underwood et al.* [2010] and depositional ages modified after *Zhao et al.* [2013] as well as depositional fans after *Pickering et al.* [2013]. Red dot marks the position of analyzed pumice clast for isotopes.

16 and 24 μm spot size using 5–8 J/cm^2 energy density at 1–5 Hz repetition rate. International standard glasses were measured every five to eight samples to monitor accuracy and silica and calcium concentrations, measured by EMP, are used as an internal standard to calibrate the trace element analyses. Average precision and accuracy estimates based on 26 replicate analyses of synthetic NIST 612 and NIST 611 standards are <10% for most elements and most monitor analyses (see supporting information Table S4). Ten individual glass shard measurements are bracketed by two to three standard measurements at the beginning and end of each analytical series. Average compositions of analyzed glasses are given in supporting information Table S2.

2.3. Isotopes

One pumice clast from the youngest Tuffaceous sandstone 1 (322-C0011B-2R-CC 9–11 cm; Figure 3 red box) was crashed into chips and cleaned for Sr, Nd, and Pb isotope analysis. Sr-Nd-Pb isotope analyses were performed on ~100 mg whole rock chips in Class 1000 clean rooms. The leached chips (2 N HCl at 70°C for 60 min and triple rinsed with ultrapure water thereafter) were weighed in Teflon beakers and digested in a solution of ultrapure concentrated HF and HNO_3 (5:1) at 150°C for 60 h. Ion chromatography was carried out following the procedures of *Hoernle et al.* [2008] and *Hoernle and Tilton* [1991]. The isotope analysis was carried out at GEOMAR using a Thermo Finnigan TRITON (Sr, Nd isotopes) and Finnigan MAT 262-RPQ2+ (Pb isotopes) thermal ionization mass spectrometers operating all in static mode. Within-run normalization factors were 0.1194 for $^{86}Sr/^{88}Sr$ and 0.7219 for $^{146}Nd/^{144}Nd$. All errors are reported as 2 sigma of the mean. NBS 987 values measured along with the sample were normalized for the analytical session to $^{87}Sr/^{88}Sr = 0.71025$ and the session specific normalization value applied to the sample data. Similarly the Nd isotope data are reported relative to La Jolla $^{143}Nd/^{144}Nd = 0.511850 \pm 0.000007$ for the TRITON. Lead isotope ratios are normalized to NBS 981 values from *Todt et al.* [1996]. The long-term reproducibility of NBS 981 measured along with the samples is $^{206}Pb/^{204}Pb = 16.899 \pm 0.007$, $^{207}Pb/^{204}Pb = 15.437 \pm 0.009$, and $^{208}Pb/^{204}Pb = 36.525 \pm 0.029$ (n = 189). Total blanks during this measuring series for Pb chemistry were <100 pg and thus are considered negligible. This sample yielded $^{87}Sr/^{86}Sr$: 0.703680 ± 0.000003, $^{143}Nd/^{144}Nd$: 0.513012 ± 0.000003, $^{206/204}Pb$:

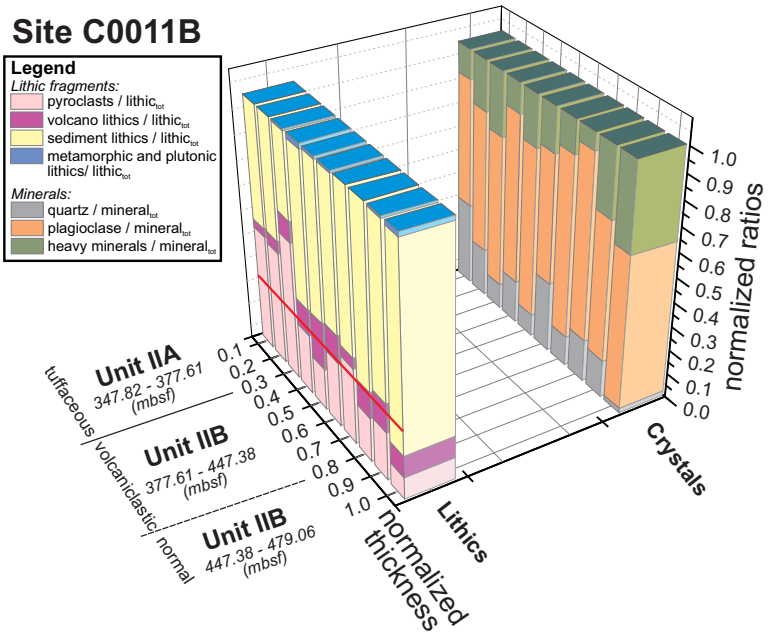

Figure 4. Smear slide petrographic data [*Underwood et al*., 2010] for Unit II versus depth (mbsf) showing the stratigraphic changes in lithic components and magmatic minerals within the subunits by criteria for division into "normal," "volcanoclastic," and "tuffaceous" sandstones. Red line indicates 25% of pyroclasts.

18.327 ± 0.000429, $^{207/204}$Pb: 15.559 ± 0.0002, and $^{208/204}$Pb: 38.364 ± 0.0008; all errors are reported as 2 sigma of the mean (supporting information Table S3).

2.4. Alteration

All microanalyses aimed at the center of glass shards because variable submarine alteration [*Kutterolf et al*., 2007] first causes elemental exchange at the surface of single glass shards. The effects of alteration are most commonly manifested as decreased iron, silica, and calcium values, as well as increased aluminum concentrations when the samples are near the top or the base of the tuffaceous sandstones [*Schindlbeck et al*., 2013]. This most probably reflects simplified interaction with seawater at sediment-sediment or sediment-water boundaries (see also experimental results in *Schacht et al*. [2008]). The rest of the tuffaceous sandstones are more preserved from alteration, probably because of poor sorting and thus closed pore-spaces. This is also reflected by average totals around 93 wt % which are normal values for marine tephras [e.g., *Kutterolf et al*., 2008, *Lowe et al*., 2008]. Nevertheless, our results are also supported by the study of *Bryant et al*. [2003] who determined average totals for Izu Bonin glasses of 90–100 wt % and no systematic relationship between age and degree of hydration, especially in Izu-Bonin tephras younger than 10 Ma.

3. Unit II and the Tuffaceous Sandstones

Lithologic Unit II, representing the newly defined "middle Shikoku Basin" sediment formation, has been divided into two subunits, IIA and IIB, based on the abundance of volcanic glass shards, mineral, and/or lithic contents (Figure 4 and Table S1) and whole-rock compositional data gathered by shipboard XRF [*Underwood et al*., 2010]. The upper subunit IIA (347.82–377.61 mbsf) consists of silty claystone and includes three 1–10 m thick interbeds of tuffaceous sandstones (TST) [cf. *Fisher and Schmincke*, 1984], characterized by high amounts (57–82%) [*Schindlbeck et al*., 2013] of pyroclasts in their modal compositions. Unit IIB (377.61–479.06 mbsf), with a silty claystone to siltstone dominated background sedimentation, shows a transition from interbedded volcaniclastic sandstones (>25% volcanic clasts) at the top to normal sandstones (<25% volcanic clasts) at the base (Figures 2 and 4).

TST 1 and 3 were not completely recovered while a complete core of the 1.75 m thickness of TST 2 is available. Of the three sandstone packages, tuffaceous sandstones 1 and 2 are single beds whereas tuffaceous sandstone 3 is composed of at least two beds (3a, 3b, top to bottom), suggesting two discrete sedimentation events [e.g., *Schindlbeck et al*., 2013].

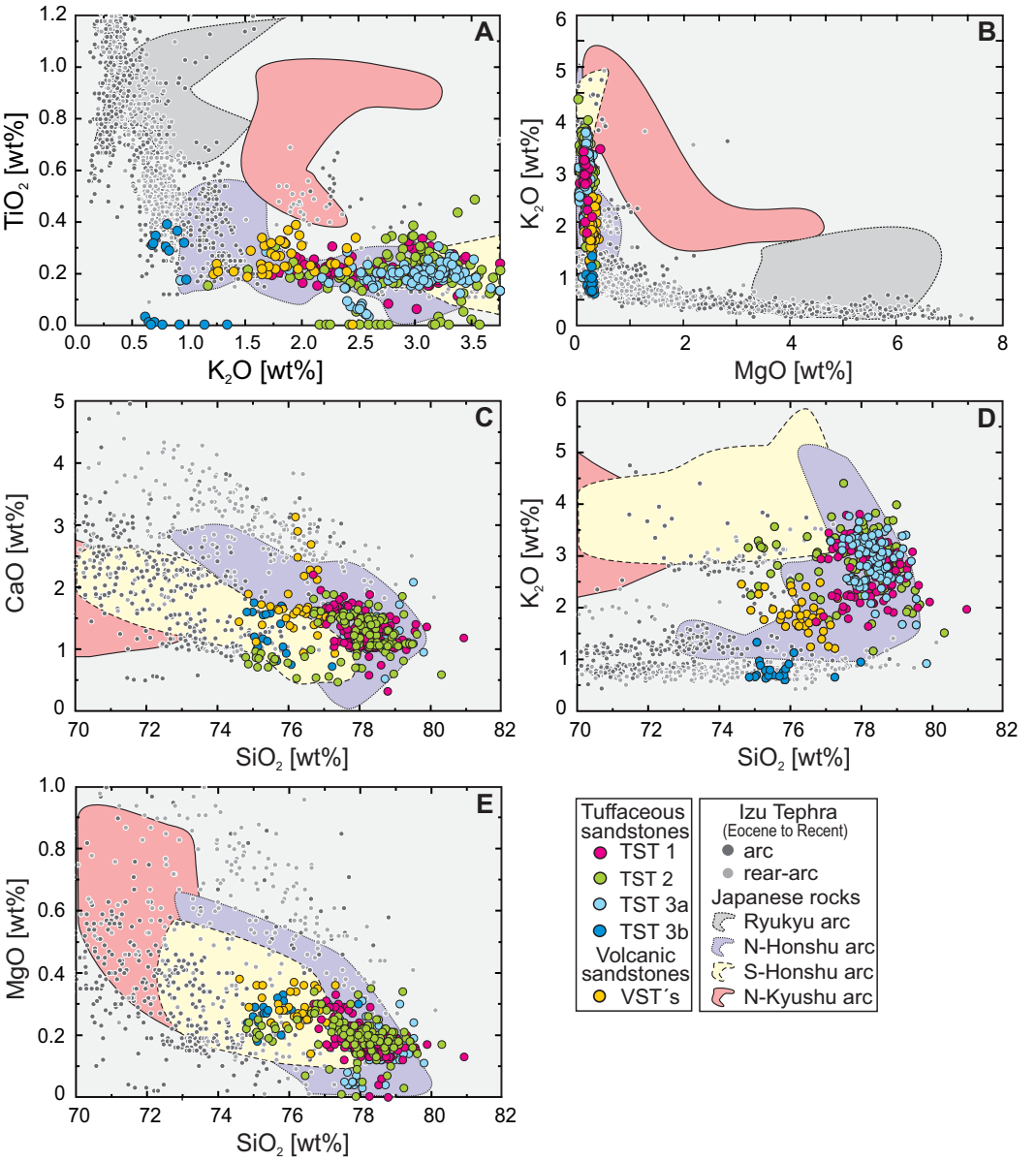

Figure 5. (a) TiO_2 versus K_2O, (b) K_2O versus MgO, (c) CaO versus SiO_2, (d) K_2O versus SiO_2, and MgO versus SiO_2 diagrams with glass shards of tuffaceous sandstone 1–3 in comparison to glass shard analysis from pumices in submarine mass flows, ashes, and on-shore tephras from Izu-Bonin arc and rear-arc after *Arculus and Bloomfield* [1992], *Bryant et al.* [2003], *Clift et al.* [2003], *Straub* [2003], *Straub et al.* [2004], and the references therein. Additionally, gray, red, blue, and yellow fields show the magmatic compositions (if available and fitting the range of the diagram) of the Japanese volcanic (paleo-)arc (Setouchi Volcanic Belt, Northern Honshu arc, and Kii peninsula at Southern Honshu arc [e.g., *Clift et al.*, 2003; *Hanyu et al.*, 2006; *Hunt and Najman*, 2003; *Kobayashi and Nakamura*, 2001; *Shinjoe et al.*, 2002, 2007; *Tatsumi*, 2006]) as well as from the Ryukyu arc [*Shinjo et al.*, 2000] and Northern Kyushu arc [*Shibata et al.*, 2013].

Petrographic and geochemical analyses constrain the interpretation of the tuffaceous sandstone beds as density-graded volcaniclastic turbidites that formed during distinct, compositionally homogeneous volcanic events, probably the entrance of massive pyroclastic flows into the ocean, as opposed to the collapse of compositionally heterogeneous continental slope sections [*Schindlbeck et al.*, 2013].

4. Provenance of the Tuffaceous Sandstones

Fresh glass shards and pumice fragments dominate the component inventory of the tuffaceous sandstones (Figures 4 and 5). They have fairly uniform major element compositions suggesting a provenance from a

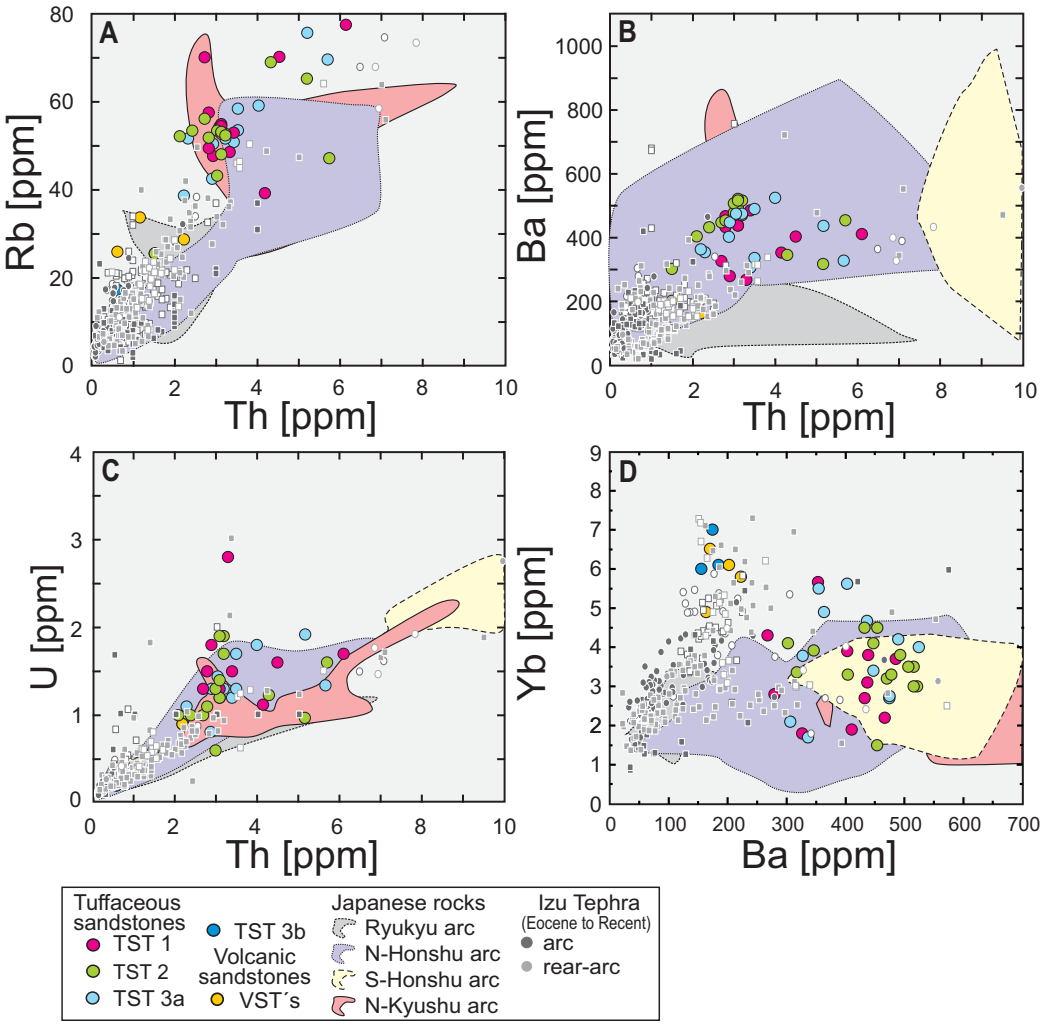

Figure 6. Trace element discrimination diagrams ((a) Rb versus Th, (b) Ba versus Th, (c) U versus Th, and (d Yb versus Ba) to distinguish between volcanics in Unit II. For comparison, the available trace elements from the literature listed in Figure 5 are shown and are complemented by data from *Arculus and Bloomfield* [1992], *Clift et al.* [2003], *Egberg et al.* [1992], *Freyer et al.* [1990], *Hiscott and Gill* [1992], *Ishizuka et al.* [2006], *Kimura et al.* [2002], *Kimura and Yoshida* [2006], *Machida et al.* [2008], *Shibata and Nakamura* [1997], *Straub et al.* [2004, 2010], *Tamura et al.* [2009], *Togashi et al.* [1992], and the references therein for the Izu-Bonin arc. Filled symbols represent the bulk rock data, unfilled glass analyses. Squares show the data in sample with <70% silica round bullets with >70% silica.

common source region. Only the lowermost tuffaceous sandstone bed (TST 3b in Figure 5) and the volcaniclastic sandstones of Unit IIb differ in their chemical composition.

In the following, we will determine correlations and miscorrelations between Unit II sandstones chemical compositions and published data for each possible provenance area. Single diagrams may not be irrevocable proofs of provenance because we cannot exclude the match of some exotic compositions to our Unit II sandstones, but considering all data, we will suggest a fairly solid provenance model for these sandstones.

4.1. Provenance of the Tuffaceous Sandstones: Major and Trace Elements

Regarding the glass compositions, our analyzed tuffaceous sandstones show moderate K_2O values (2.1–3.3 wt %), low MgO (0.16–0.33 wt %), FeO (1.16–1.6 wt %), CaO (1.16–1.88 wt %), and high silica (77.59–78.95 wt %) contents. The major-element compositions of pyroclasts of the younger sandstones TST 1, 2, and 3a differ slightly between each other but mostly from typical Izu-Bonin volcanic arc and rear-arc glass compositions particularly in K_2O and TiO_2 [data from *Arculus and Bloomfield*, 1992; *Bryant et al.*, 2003; *Clift et al.*, 2003; *Straub*, 2003; *Straub et al.*, 2004] (Figure 5a). In contrast, older TST 3b and volcaniclastic sandstones of Unit IIb show a much clearer match to the Izu-Bonin compositional fields in Figure 5a.

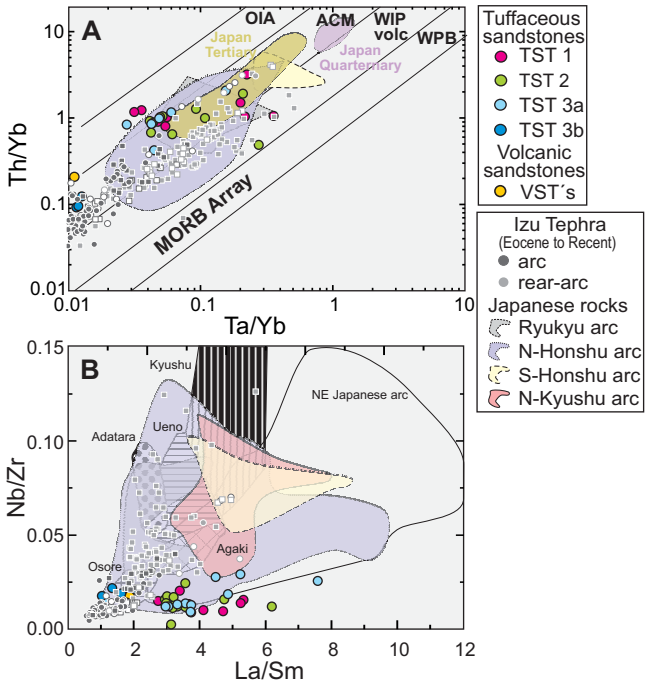

Figure 7. Trace element ratio ((a) Th/Yb versus Ta/Yb [*Gorton and Schandl*, 2000] and (b) Nb/Zr versus La/Sm [*Clift et al*., 2003]) plots indicating different Japanese and Izu-Bonin provenances in comparison with the Unit II sandstone results. (a) Provenance fields for Tertiary and Quaternary Japanese arc rocks are modified from *Gorton and Schandl* [2000]; OIA, ocean island arc; ACM, active continental margin; WIPvolc, within plate volcanics; and WPB, within plate basalts. (b) Shaded fields represent data from NE Japan arc volcanoes Osore, Akagi, Nekoma, and Ueno modified after *Clift et al*. [2003] and NE Japanese marine Arc tephras from IODP Site 1151 from *Clift et al*. [2003]. For comparison, the available trace elements from the literature listed in Figures 5 and 6 are shown. Regarding IBM data, filled symbols represent the bulk rock data, unfilled glass analyses. Squares show the data in sample with <70% silica round bullets with >70% silica.

The same can be seen when considering also the evolved bulk rock compositions from the Izu-Bonin arc or rear-arc [e.g., *Egberg et al*., 1992; *Freyer et al*., 1990; *Hiscott and Gill*, 1992; *Ishizuka et al*., 2006; *Machida et al*., 2008; *Nishimura et al*., 1992; *Straub and Layne*, 2003; *Straub et al*., 2010; *Tamura et al*., 2009; *Tani et al*., 2008] and also elements such as K_2O, CaO, MgO, and SiO_2 (Figures 5b–5e). In general, we cannot exclude an overlap with major element contents from our tuffaceous sandstones, but (1) the overlap is fairly small regarding the younger tuffaceous sandstones 1, 2, and 3a and (2) only TST 3b and the volcaniclastic sandstones show stronger overlapping especially with Izu-Bonin rear arc compositions.

However, the younger tuffaceous sandstones (and partly sandstones from TST 3b and Unit IIb) overlap better with magmatic compositions of the Japanese volcanic (paleo-)arc (data from Setouchi Volcanic Belt, Northern Honshu arc, and Kii peninsula at Southern Honshu arc [e.g., *Clift et al*., 2003; *Hanyu et al*., 2006; *Hunt and Najman*, 2003; *Kimura and Yoshida*, 2006; *Kobayashi and Nakamura*, 2001; *Shinjoe et al*., 2002, 2007; *Tatsumi*, 2006]). If available, provenance fields for the Ryukyu arc and Northern Kyushu arc, based on data from *Shinjo et al*. [2000] and *Shibata et al*. [2013], respectively, clearly mismatch the data from all tuffaceous sandstones.

Trace element contents (e.g., Rb, Th, U, Ba, Yb; Figures 6a–6d) show better that our data can be separated into two groups: a "young" sandstone group, defined by samples from tuffaceous sandstone 1 to 3a and an "old" sandstone group defined by samples from the volcaniclastic sandstones of Unit IIB and TST 3b. Confirming the results from major element chemistry, this suggests that at least two, probably temporally distinguishable, source areas were tapped by the sandstones of Unit II.

Comparison to the provenance fields of Ryukyu, Kyushu, and Honshu arc as well as Izu-Bonin arc and rear-arc reveal no clear correlations between these potential source areas and the younger tuffaceous sandstones (Figure 6).

However, Northern Kyushu arc and Northern Honshu arc data fields, where available, seem to be the best approximation for a possible source area of the younger TST sandstones (Figure 6). In contrast, we observe that samples from TST 3b and the volcaniclastic sandstones of Unit IIb are similar to the Izu-Bonin rear-arc data and different from the Izu-Bonin arc data and from the other arc provenance fields (Figure 6).

4.2. Limitations in Provenance Study Regarding Major and Trace Elements

Comparing major and trace element compositions of the different Unit II sandstones with data from potential source areas in that region indicate that compositions commonly overlap to varying degrees. Some of this overlap may reflect different analytical techniques in the literature, as the lack of Late Miocene glass

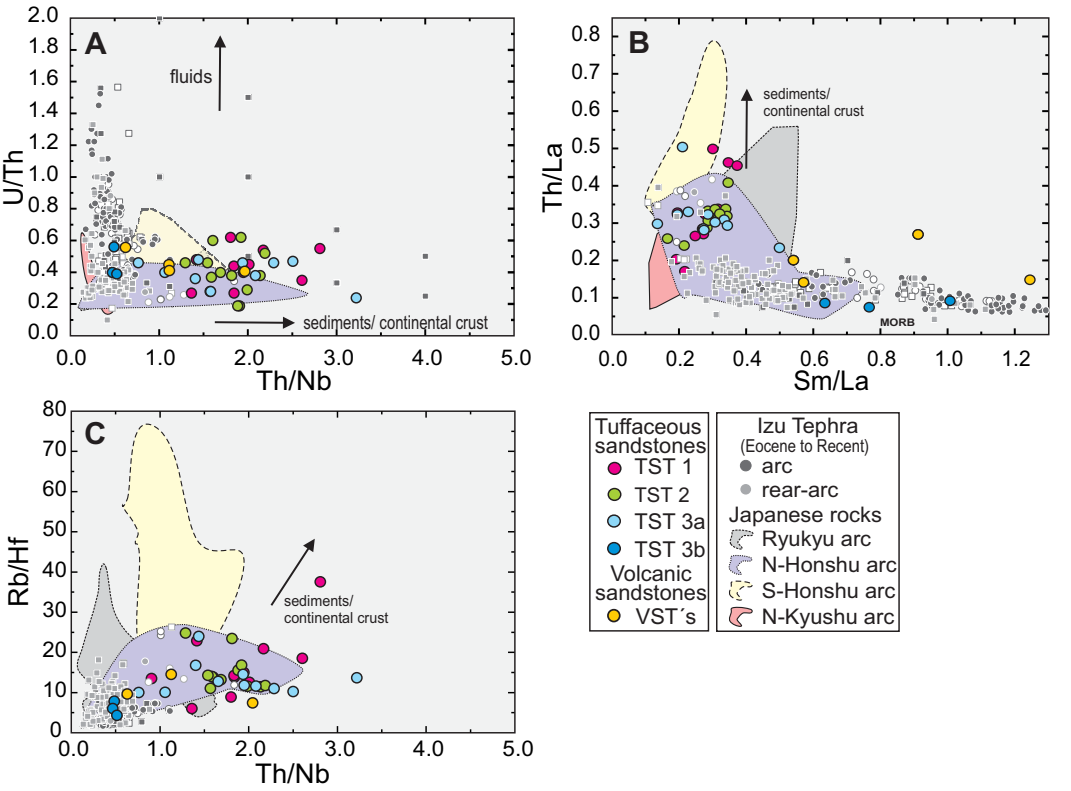

Figure 8. Trace element ratio diagrams after literature (a = *Bryant et al.* [2003]; b = *Plank* [2005]; and C = *Hannah et al.* [2002] and *Bryant et al.* [2003]) indicating different influences to source areas by continental crust interaction or the respective sediment signal from the slab or a fluid in comparison to the analyzed tuffaceous sandstones of this study. Data from the original authors are complemented by data for IBM and Japanese (paleo) arcs referenced in Figures 5 and 6. Regarding IBM data, filled symbols represent the bulk rock data, unfilled glass analyses. Squares show the data in sample with <70% silica round bullets with >70% silica.

data in the literature necessitates comparison to bulk rock data of evolved and more primitive tephras, lavas, and younger rocks.

Surprisingly, the partly heterogenic comparative data sets from literature (volcanic complexs, volcanoes, or arc segments) do not differ significantly from each other at one source, although the respective used analytics and/or grade of differentiation of analyzed samples within this provenance field in this literature data often varies (often a mixture of data from highly evolved and primitive rocks as well as lava (bulk rock) and tephras (glass), due to the limited available data in the literature). Therefore, they are still suitable for our provenance study regarding our basic correlation to general arc provinces, and not to specific volcanic centers.

Available samples in Unit II sediments do not allow to constrain the amount of fractional crystallization that may have affected the primary magma and thus the enrichment of compatible and incompatible elements of the evolved magmas that generated the pyroclasts contained in the tuffaceous sandstones. Ideally, mafic equivalents of our deposits would help us to evaluate the effect of differentiation on the resulting tuffaceous sandstone magmas. Since we do not have those samples we use trace elements and especially trace element ratios that are not significantly changed by differentiation processes to evaluate the provenance signatures. Although we cannot completely rule out the effect of some crystal fractionation, Nb/Zr ratios, for example, could be widely changed by zircon but it is not often observed in the pumice clasts of Unit II, we consider the trace element ratios as our best tool to unravel the provenance of our tuffaceous sandstones.

4.3. Provenance of the Tuffaceous Sandstones: Trace Element Ratios

With this limitation in mind, a Th/Yb versus Ta/Yb diagram allows to distinguish between Quaternary and Tertiary magmatic compositions from the Japanese mainland [*Gorton and Schandl*, 2000]. Including also the Izu-Bonin arc and rear-arc data used in the previous diagrams, Figure 7a shows that Unit II pyroclast compositions largely overlap with the Japanese Tertiary field, in agreement with the sandstones ages (Figure 1).

Similarly, the sandstone data overlap with the Japanese arc in a Nb/Zr versus La/Sm space (Figure 7b). The previously used Kyushu, Ryukyu, N-Honshu, and S-Honshu (Kii) arc data mimic completely the more general provenance fields shown by *Clift et al*. [2003]. In both diagrams, however, the lowermost tuffaceous sandstone (TST 3b) and volcanic sandstones from Unit IIB differ again from the younger TSTs by overlapping, or lying close to the Izu-Bonin data.

4.4. Provenance of the Tuffaceous Sandstones: Continental Signal

Izu-Bonin lavas have a strong signature from aqueous fluids released by the slab [*Straub and Layne*, 2003] while Japanese mainland has experienced melting of sediment or crustal assimilation or anything that gives a crustal signature [e.g., *Stern et al*., 2003]. Elevated values of Th/La, Rb/Hf, and Th/Nb (Figure 8), therefore, suggest an influence of continental crust or subducted terrigeneous sediment on the magmatic compositions [e.g., *Hannah et al*., 2002; *Bryant et al*., 2003], whereas elevated values of U/Th and Ba/La indicate an influence by pelagic sediments or fluids that had equilibrated with them [e.g., *Carr et al*., 2007; *Patino et al*., 2000]. Thus, high U/Th at low Th/Nb in Izu-Bonin arc data (Figure 8a) suggests a strong influence of pelagic sediment-derived fluids on Izu-Bonin magmatic compositions [cf. *Straub and Layne*, 2003] that seems to be shared by pyroclast compositions of TST 3b and volcanic sandstones of Unit IIB. Pyroclasts of the other sandstones, however, have elevated Th/Nb at low U/Th and thus are probably derived from a magmatic source that was influenced by terrigeneous sediment or continental crust (Figure 8a).

The same distinction can be made if looking to a Th/La versus Sm/La or Rb/Hf versus Th/Nb diagrams where Rb/Hf and Th/La ratios are proxies for a continental source influence (Figures 8b and 8c). Higher Sm/La values are found in the Izu-Bonin data that are probably more affected by MORB-like crust and show similarities to TST 3b and the volcaniclastic sandstones of Unit IIb (Figure 8b).

In contrast to this rather clear correlations of tuffaceous sandstone 3b and Unit IIb volcaniclastic sandstones to the Izu-Bonin (rear-)arc source, the compositions of the younger tuffaceous sandstone beds 1 to 3a overlap partly with data from the continental Quaternary and Miocene Japanese arc (Figure 8 and references in caption of Figures 5 and 6). Opposed to the Japanese mainland [e.g., *Stern et al*., 2003; *Isozaki et al*., 2010], there is neither continental crust nor trench sediment of continental composition at the Izu-Bonin arc, which therefore also supports our interpretation that the Izu-Bonin arc is not a likely source region for the tuffaceous sandstones TST 1, 2, and 3a, which have high Th/Nb, Th/La, and Rb/Hf values. The minor differences in trace element ratios between the individual younger TST beds most probably indicates different eruptions of the same (or if different, then regionally related) eruptive centers, an interpretation that is in agreement with *Schindlbeck et al*. [2013].

Our interpretation is further supported by the work of *Stern et al*. [2003] who summarized the evolution of the IBM as being a good example of intraoceanic convergent margins that are built on oceanic crust, in contrast to island arcs originating on continental crust (e.g., Japanese arc systems or the Andes). In the case of the IBM, the collision of the IBM with the continental Honshu arc has taken place since 15 Ma [*Stern et al*., 2003] and may have influenced the magmatic compositions. Nevertheless, strong compositional differences between modern IBM tephras and other arc systems in that region have existed over most of the arc's history, with northern IBM being more depleted and southern IBM being relatively enriched [*Stern et al*., 2003]. In contrast, *Tamura et al*. [2009] claimed that there are also some indications of continental crust-influenced rocks (rhyolites) from Izu-Bonin arc volcanoes due to partial melting of the middle crust (tonalite) that can be found in Late Quaternary tephra compositions and that there are some temporal changes between Tertiary and Quaternary volcanic rocks from IBM.

We cannot exclude the possibility that some exotic volcanic products from IBM may show a continental signature similar to that of the palaeo-Honshu arc and that they may be correlative to our younger tuffaceous sandstone compositions. But since *Tamura et al*. [2009] restricted the occurrence of those special rhyolites from the IBM to the Quaternary and our tuffaceous sandstones are from the Miocene we are confident in our interpretation that the younger Miocene tuffaceous sandstones (1, 2, and 3a) originated from a crustal-like Japanese arc source.

4.5. Provenance of the Tuffaceous Sandstones: Far Travelled Volcanics

To summarize the chemical and sedimentological data, we posit that the tuffaceous sandstone 3 comprises one turbidite with an Izu-Bonin chemical signature (TST 3b) and another with a Japan arc signature (TST 3a)

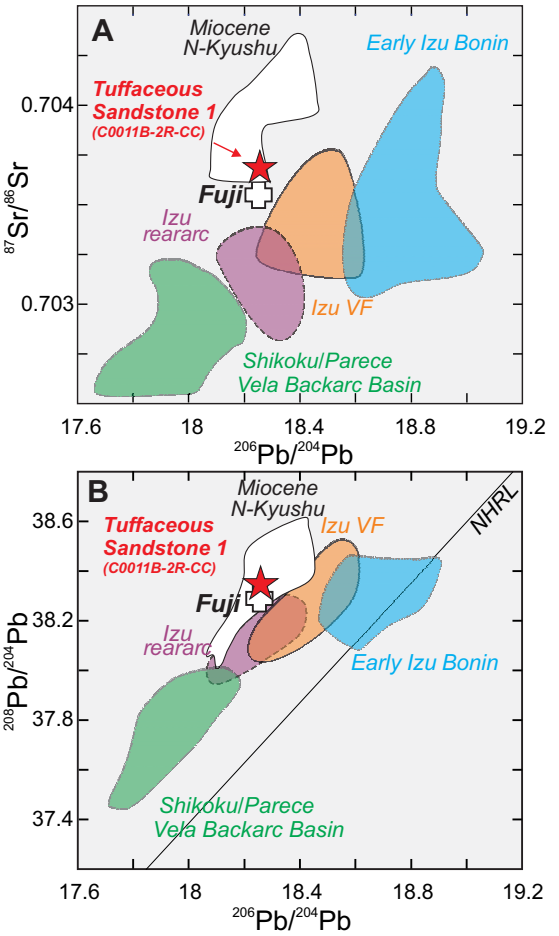

Figure 9. Lead and strontium isotope ratios (a) as well as $^{208/204}$lead and $^{206/204}$lead isotope ratios (b) of a pumice sample from tuffaceous sandstone 1 (see Figures 2 and 3) in comparison to provenance fields [*Straub et al.*, 2004] indicating Izu arc and rear arc compositions, Shikoku/Oarece Vela Backarc Basin compositions as well as data from Miocene NE Japanese rocks (white field) and Fuji (white cross) [*Nakamura et al.*, 2008; *Watanabe et al.*, 2006] volcano located in the vicinity of the collision zone between Izu arc and Honshu arc. Two sigma errors are below symbol size. Northern Hemisphere reference line (NHRL) is after *Hart* [1984].

that prevailed for the subsequent sandstones. Thus, TST 3a and TST 3b most probably derived from distinct source regions (IBM versus Japanese mainland) and judging from lithological structures and grain sizes [*Underwood et al.*, 2010], both seem to have traveled similar distances from their sources. We therefore favor a deposition site where both geochemical signatures were available within a plausible distance (10s to 100s kilometers) [e.g., *Schindlbeck et al.*, 2013] from their volcanic source. Only the wider region around the collision zone between the Izu arc and the Japanese paleo-arc (represented today by the Izu Peninsula on Japanese mainland) facilitated the tapping of both volcanic sources.

This hypothesis is consistent with the plate tectonic reconstruction by *Pickering et al.* [2013]. Additional supportive evidence comes from isotope analysis of a pumice fragment from tuffaceous sandstone 1. While admittedly only a single analysis, tuffaceous sandstone 1 shows less radiogenic ^{206}Pb/^{204}Pb values for similar ^{87}Sr/^{86}Sr isotopic compositions compared to Izu-Bonin arc and rear arc tephras [*Straub et al.*, 2004], but equal the ^{206}Pb/^{204}Pb, ^{208}Pb/^{204}Pb, and ^{87}Sr/^{86}Sr ratios of the Miocene N-Kyushu rocks or modern Fuji volcano [*Gust et al.*, 1997; *Nakamura et al.*, 2008; *Watanabe et al.*, 2006], which is part of the Honshu volcanic front in the vicinity (<100 km) of today's Izu Peninsula (Figure 9).

Unit IIB, underlying the tuffaceous sandstones of Unit IIA, is much more heterogeneous in lithology and chemical composition. It is mainly composed of sedimentary clasts that are associated with upward increasing fractions of volcanic glasses that have distinct major and trace element compositions compared to the tuffaceous sandstones of Unit IIA (Figures 4–6 and Table S2). Thus, there is a change in provenance from Unit IIB to IIA. Within lowermost IIA, we have demonstrated a change in provenance from tuffaceous sandstone beds 3b to 3a. Unit TST 3b, which shows similarities to glass shards present in the volcaniclastic sandstones of Unit IIB, represents the last occurrence of an Izu-Bonin geochemical signature at site. Using sediment accumulation rates of 6 cm/kyr estimated for this time interval at Site C0011 [*Underwood et al.*, 2010], we calculate an age between 7.8 and 8.3 Ma. We interpret that this age of TST 3b possibly also constrains the onset of a new collision phase between the Izu-Bonin arc and the Japanese paleo-arc, which would be consistent with a depositional area between Izu-Bonin and Honshu arc [*Pickering et al.*, 2013; *Mahony et al.*, 2011].

The compilation of provenance results from major and trace element chemistry, isotopic ratios, comparison to correlative data from geologically feasible and available source areas, strongly suggests an origin of the

younger tuffaceous sandstones 1 to 3a from the paleo-Honsu arc, and from the Izu-Bonin arc for TST 3b. We note, however, that we sensu stricto cannot rule out the tuffaceous sandstones 1 to 3a as originating from an Izu-Bonin source although, in our opinion, the majority of the compiled evidence supports our interpretation. Indeed, the evidence from mineral chemistry and the differences in sedimentology described by *Schindlbeck et al.* [2013] additionally favors this suggestion. Our interpretation is also the most consistent with the regional perspective to match both larger source areas (within a wide regionally range allowing also an origin from the regular paleo-Honshu arc) in one depositional area.

While future research, especially regarding different compositions from the different source areas, may give further constraints and answers to this discussion, the possibility of a paleo-Honshu source, not necessarily within the collision zone itself but in the hinterland, is additionally supported by other lines of evidence, including:

1. The numerous (∼100) Late Miocene calderas available at the NE-Honshu arc, with the most southern one located only ∼150 km from the coastline at the IBM-Honshu arc collision zone [*Acocella et al*., 2008; *Yoshida*, 2001], where the subaerial pyroclastic flows have been transferred into the submarine pyroclastic turbidities travelling to the final depositional area.

2. Similar potassium versus silica compositions in the similar time range (8 Ma) [*Acocella et al*., 2008].

3. *Kimura and Yoshida* (2006) assist the crustal signature of the Quaternary NE-Honshu magmas and the resulting provenance fields correlates best with our tuffaceous sandstones, as well as

4. Comparable younger (4 Ma) ignimbrite sheets (ZNp tephra) spanning 600 km southwest to northeast over central Japan, being sourced somewhere in the central Honshu region and traveled to Boso peninsula in the Izu-arc-paleo Honshu arc collision zone [*Allen et al*., 2012].

5. Submarine Volcaniclastic Turbidite Sheets

Three long-lived submarine depositional systems have contributed to the basin evolution of the Shikoku Basin [*Pickering et al*., 2013]. Sediments of Unit IIB were deposited in channels of the older so called Daiichi Zenisu Fan, while the younger Daini Zenisu Fan, that has a sheet-like geometry, contains the thick-bedded and coarse-grained tuffaceous sandstones of Unit IIA (e.g., Figure 3). Given that the palaeo-Honshu arc around today's Izu Peninsula is the most plausible source region of the tuffaceous sandstones, their depositing density currents, which originated from pyroclastic flows on land [*Schindlbeck et al*., 2013], must have travelled ∼300 km to reach Site C0011 of Expedition 322 [e.g., Figure 1].

With these geometric constraints, we can estimate the volume of the tuffaceous sandstone beds in order to characterize the magnitude of their parental volcanic eruptions and to demonstrate the impact of these sheet-like deposits on the region. However, the exact geometry of the deposits is unknown and we thus use three scenarios for minimum, conservative, and moderate volume. The minimum case assumes the sandstones are entirely confined to 1 km wide channels along which their thickness decreases with distance from their source (∼300 km travel distance) due to continuous sedimentation such that the thickness at Site C0011 is one third the initial thickness. Strong channeling, however, does not fit the seismically constrained sheet-like shape of the younger Daini Zenisu Fan [*Pickering et al*., 2013]. The conservative and medium cases refer to a sheet-like geometry with sheet widths of 10 and 25 km, respectively; the thickness decay with distance is the same as for the minimum case. The total deposit volumes (Vt) are converted to dense-rock equivalent (DRE) magma volumes (Vm) using the function

$$V_m = V_t j(p\rho_p + c\rho_c)\frac{1}{\rho_m}$$

where j = 0.75 is the mass fraction of juvenile pyroclastics in the sandstone, p is the mass fraction of pumice/glass shards in the juvenile fraction, c is the mass fraction of crystals in the juvenile fraction, ρ_p = pumice/glass density, ρ_c = crystals density, and ρ_m = density of vesicle-free magma. The resulting DRE magma volumes are ∼0.5 km^3 for each tuffaceous sandstone bed for the minimum case, and ∼5 and ∼17 km^3 for the conservative and medium scenarios, respectively, and speak to the potentially large size of the responsible volcanic eruptions.

6. Summary

The "middle Shikoku Basin" sediment succession encompasses a lower subunit IIB with an Izu-Bonin arc source and an upper subunit IIA that contains three packages of tuffaceous sandstones (TST 1–3), which are dominated by compositionally homogeneous pyroclastic material derived from distinct eruptive events. Comparison of characteristic magmatic trace element ratios for potential source regions constrains a most likely provenance of the sandstones in the hinterland of the former collision zone between Izu-Bonin and Japanese paleo-arcs, although a single source area at the Izu-Bonin arc or the paleo-Honshu arc cannot be completely excluded. While the composition of the lowermost TST 3b has an Izu-Bonin signature, compositions of the overlying sandstones have a trace-element signature typical of the Japanese continental arc.

These compositional signatures support the interpretation that the depositional area of the investigated sandstone beds tapped both arc systems between 7.6 and 8.3 Ma. From ~7.8 Ma on until almost 7.6 Ma, at least three large-volume eruptions, most probably ignimbrite-forming and discharging at least ~0.5 to 13 km^3 (DRE) of magma, have occurred only at the source region on the Japanese mainland. These wide and voluminous distributions of the tuffaceous sandstones on the surface of the Philippine Plate have the potential to also affect the subduction processes regionally, with regard to alteration processes, pore water chemistry, and sediment composition.

Acknowledgments

This research used samples and/or data provided by the Integrated Ocean Drilling Program (IODP). We want to thank the German Research Foundation to support this study by the grant KU 2685/1-1. We appreciate the great help of Jan Fietzke and Edmund Hathorne during the first La-ICPMS analyses with the quadropole LA-ICPMS shortly before the AGU and together with Matthias Frische and Dagmar Rau the subsequent measurements in the new LA-ICPMS laboratory of GEOMAR. Special thanks go to Folkmar Hauff for providing the isotope labs at GEOMAR. Partial funding for this research was provided by USAC postcruise support to R. W. Murray on behalf of R. P. Scudder for Expeditions 322 and 333. Research also supported by U.S. National Science Foundation grant OCE-0958002 to R. W. Murray.

References

Acocella, V., T. Yoshida, R. Yamada, and F. Funiciello (2008), Structural control on late Miocene to Quaternary volcanism in the NE Honshu arc, Japan, *Tectonics*, *27*, TC5008, doi:10.1029/2008TC002296.

Allen, S. R., A. Freundt, and K. Kurokawa (2012), Characteristics of submarine pumice-rich density current deposits sourced from turbulent mixing of subaerial pyroclastic flows at the shoreline: Field and experimental assessment, *Bull. Volcanol.*, *74*, 657–675.

Arculus, R. J., and A. L. Bloomfield (1992), Major-element geochemistry of ashes from Sites 782, 784, and 786 in the Bonin Forearc, in *Proceedings of the Ocean Drilling Program, Scientific Results*, edited by P. Fryer et al., pp. 277–292, Ocean Drill. Program, College Station, Tex.

Bryant, C. J., R. J. Arculus, and S. M. Eggins (2003), The geochemical evolution of the Izu-Bonin arc system: A perspective from tephras recovered by deep-sea drilling, *Geochem. Geophys. Geosyst.*, *4*(11), 1094, doi:10.1029/2002GC000427.

Carr, M. J., L. C. Patino, and M. D. Feigenson (2007), Petrology and geochemistry of lavas, in *Central America—Geology, Resources and Hazards*, edited by J. Buntschuh and G. E. Alvarado, A. A. Balkema, Rotterdam, Netherlands.

Clift, P. D., G. D. Layne, Y. M. R. Najman, A. Kopf, N. Shimizu, and J. Hunt (2003), Temporal evolution of boron flux in the NE Japan and Izu arcs measured by ion microprobe from the forearc tephra record, *J. Petrol.*, *44*(7), 1211–1236.

Egeberg, P. K., A. O. Brunfelt, and A. S. Stabel (1992), Characterization and correlation of megascopic tephras in Site 792 cores from the Izu-Ogasawara forearc basin (Japan) by trace elements and 87Sr/86Sr and 143Nd/144Nd isotopes, in *Proceedings of the Ocean Drilling Program, Science Results*, vol. 126, edited by B. Taylor et al., pp. 457–465, Ocean Drill. Program, College Station, Tex., doi:10.2973/odp.proc.sr.126.149.

Expedition 333 Scientists (2011), NanTroSEIZE Stage 2: Subduction inputs 2 and heat flow, *Prelim. Rep. Integrated Ocean Drill. Program*, *333*, 107 pp., doi:10.2204/iodp.pr.3332011.

Fisher, R. V., and H.-U. Schmincke (1984), *Pyroclastic Rocks*, 472 pp., Springer, Berlin.

Fryer, P., B. Taylor, C. H. Langmuir, and A. G. Hochstaedter (1990), Petrology and geochemistry of lavas from the Sumisu and Torishima backarc rifts, *Earth Planet. Sci. Lett.*, *100*, 161–178.

Gorton, M. P., and E. S. Schandl (2000), From continents to island arcs: A geochemical index of tectonic setting for Arc-related and within-plate felsic to intermediate volcanic rocks, *Can. Mineral.*, *38*, 1065–1073.

Gust, D. A., R. J. Arculus, and A. B. Kersting (1997), Aspect of magma sources and processes in the Honshu arc., *Can. Mineral.*, *35*, 347–365.

Hannah, R. S., T. A. Vogel, L. C. Patino, G. E. Alvarado, W. Perez, and D. R. Smith (2002), Origin of silicic volcanic rocks in central Costa Rica: A study of a chemically variable ash-flow sheet in the Tiribi Tuff, *Bull. Volcanol.*, *64*, 117–133.

Hanyu, T., Y. Tatsumi, S. Nakai, Q. Chang, T. Miyazaki, K. Sato, K. Tani, T. Shibata, and T. Yoshida (2006), Contribution of slab melting and slab dehydration to magmatism in the NE Japan arc for the last 25 Myr: Constraints from geochemistry, *Geochem. Geophys. Geosyst.*, *7*, Q08002, doi:10.1029/2005GC001220.

Hart, S. R. (1984), A large-scale isotope anomaly in the Southern Hemisphere mantle, *Nature*, *309*, 753–757.

Hiscott, R. N., and J. B. Gill (1992), Major and trace element geochemistry of Oligocene to Quaternary volcaniclastic sands and sandstones from the Izu-Bonin arc, in *Proceedings of the Ocean Drilling Program, Science Results*, vol. 126, edited by B. Taylor et al., pp. 467–485, Ocean Drill. Program, College Station, Tex., doi:10.2973/odp.proc.sr.126.150.

Hoernle, K., et al. (2008), Arc-parallel flow in the mantle wedge beneath Costa Rica and Nicaragua, *Nature*, *451*, 1094–1097.

Hoernle, K. A., and G. R. Tilton (1991), Sr-Nd-Pb isotope data for Fuerteventura (Canary Islands) basal complex and subaerial volcanics: Applications to magma genesis and evolution, *Schweiz. Mineral. Petrogr. Mitt.*, *71*, 3–18.

Hunt, J. B., and P. G. Hill (2001), Tephrological implications of beam size—Sample-size effects in electron microprobe analysis of glass shards, *J. Quat. Sci.*, *16*(2), 105–117.

Hunt, J. B., and Y. M. R. Najman (2003), Tephrochronological and tephrostratigraphical potential of Pliocene-Pleistocene volcaniclastic deposits in the Japan Forearc, in *Proceedings of the Ocean Drilling Program, Scientific Results*, vol. 186, edited by K. Suyehiro et al., Ocean Drill. Program College Station, Tex., 1–29 pp., doi:10.2973/odp.proc.sr.186.107.2003.

Ishizuka, O., et al. (2006), Early stages in the evolution of Izu-Bonin arc volcanism: New age, chemical, and isotopic constraints, *Earth Planet. Sci. Lett.*, *250*, 385–401.

Isozaki, Y., K. Aoki, N. Nakaaki, and S. Yanai (2010), New insight into a subduction-related orogen: A reappraisal of the geotectonic framework and evolution of the Japanese Islands, *Gondwana Res.*, *18*, 82–105.

Kimura, J.-I., W. I. Manton, C.-H. Sun, S. Iizumi, T. Yoshida, and R. J. Stern (2002), Chemical diversity of the ueno basalts, Central Japan: Identification of mantle and crustal contributions to arc basalts, *J. Petrol.*, *43*(10), 1923–1946.

Kimura, J.-I., and T. Yoshida (2006), Contributions of slab fluid, mantle wedge and crust to the origin of quaternary lavas in the NE Japan Arc, *J. Petrol.*, *47*(11), 2185–2322.
Kobayashi, K., and E. Nakamura (2001), Geochemical evolution of Akagi Volcano, NE Japan: Implications for interaction between island-arc magma and lower crust, and generation of isotopically various magmas, *J. Petrol.*, *42*(12), 2303–2331.
Kobayashi, K., S. Kasuga, and K. Okino (Eds.) (1995), *Shikoku Basin and its Margins*, pp. 381–405, Plenum, New York.
Kutterolf, S., U. Schacht, H. Wehrmann, A. Freundt, and T. Mörz (2007), Onshore to offshore tephrostratigraphy and marine ash layer diagenesis in Central America, in *Central America—Geology, Resources and Hazards*, edited by J. Buntschuh and G. E. Alvarado, pp. 395–423, A. A. Balkema, Lisse, Netherlands.
Kutterolf, S., A. Freundt, W. Peréz, T. Mörz, U. Schacht, H. Wehrmann, and H.-U. Schmincke (2008), The Pacific offshore record of Plinian arc volcanism in Central America, part 1: Along-arc correlations, *Geochem. Geophys. Geosyst.*, *9*, Q02S03, doi:10.1029/2007GC001631.
Kutterolf, S., A. Freundt, and C. Burkert (2011), Eruptive history and magmatic evolution of the 1.9 kyr Plinian dacitic Chiltepe Tephra from Apoyeque volcano in west-central Nicaragua, *Bull. Volcanol.*, *73*(7), 811–831.
Lowe, D. J., P. A. R. Shane, B. V. Alloway, and E. M. Newnham (2008), Fingerprints and age models for widespread New Zealand tephra marker beds erupted since 30,000 years ago: A framework for NZ-INTIMATE, *Quat. Sci. Rev.*, *27*, 95–126.
Machida, S., T. Ishii, J.-I. Kimura, S. Awaji, and Y. Kato (2008), Petrology and geochemistry of cross-chains in the Izu-Bonin back arc: Three mantle components with contributions of hydrous liquids from a deeply subducted slab, *Geochem. Geophys. Geosyst.*, *9*, Q05002, doi:10.1029/2007GC001641.
Mahony, S. H., L. M. Wallace, M. Miyoshi, P. Villamor, R. S. J. Sparks, and T. Hasenaka (2011), Volcano-tectonic interactions during rapid plate-boundary evolution in the Kyushu region, SW Japan, Japan, *Geol. Soc. Am. Bull.*, *123*, 2201–2223.
Nakamura, H., H. Iwamori, and J.-I. Kimura (2008), Geochemical evidence for enhanced fluid flux due to overlapping subducting plates, *Nat. Geosci.*, *1*, 380–384.
Nishimura, A., K. S. Rodolfo, A. Koizumi, J. Gill, and K. Fujioka (1992), Episodic deposition of Pliocene-Pleistocene pumice from the Izu-Bonin arc, Leg 126, *Proc. Ocean Drill. Program Sci. Results*, *126*, 3–21.
Patino, L. C., M. Carr, and M. D. Feigenson (2000), Local and regional variations in Central American arc lavas controlled by variations in subducted sediment input, *Contrib. Mineral. Petrol.*, *138*, 256–283.
Pickering, K. T., M. B. Underwood, S. Saito, H. Naruse, S. Kutterolf, R. Scudder, J.-O. Park, G. F. Moore, and A. Slagle (2013), Depositional architecture, provenance, and tectonic/eustatic modulation of Miocene submarine fans in the Shikoku Basin: Results from Nankai Trough Seismogenic Zone Experiment, *Geochem. Geophys. Geosyst.*, *14*, 1722–1739, doi:10.1002/ggge.20107.
Plank, T. (2005), Constraints from Thorium/Lanthanum on sediment recycling at subduction zones and the evolution of the continents, *J. Petrol.*, *46*, 921–944.
Schacht, U., S. Kutterolf, K. Wallmann, and M. Schmidt (2008), Volcanogenic sediment-seawater interactions and the geochemistry of pore waters, *Chem. Geol.*, *249*, 321–328.
Schindlbeck, J. C., S. Kutterolf, A. Freundt, R. P. Scudder, K. T. Pickering, and M. R. Wurray (2013), Emplacement processes of submarine volcaniclastic mass flow deposits (IODP Site C0011, Nankai Trough), *Mar. Geol.*, *343*, 115–124, doi:10.1016/j.margeo.2013.06.017.
Seno, T., S. Stein, and A. E. Gripp (1993), A model for the motion of the Philippine Sea Plateconsistent with NUVEL-1 and geological data, *J. Geophys. Res.*, *98*(B10), 17,941–17,948.
Shibata, T., and E. Nakamura (1997), Across-arc variations of isotope and trace element compositions from Quaternary basaltic volcanic rocks in northeastern Japan: Implications for interaction between subducted oceanic slab and mantle wedge, *J. Geophys. Res.*, *102*(B4), 8501–8064.
Shibata, T., M. Yoshikawa, J. Itoh, O. Ujike, M. Miyoshi, and K. Takemura (2013), Alomg-arc geochemical variations in Quaternary magmas of northern Kyushu Island, Japan, in *Orogenic Andesites and Crustal Growth*, edited by A. Gómez-Tuena et al., Geol. Soc. London Spec. Publ., U. K., 1–15 pp., doi:10.1144/SP385.13.
Shinjo, R., J. D. Woodhead, and J. M. Hergt (2000), Geochemical variation within the northern Ryukyu Arc: Magma source compositions and geodynamic implications, *Contrib. Mineral. Petrol.*, *140*, 263–282.
Shinjoe, H., Y. Orihashi, T. Sumii, and S. Nakai (2002), Bulk rock chemistry of the Muro pyroclastic flow deposit: A clue to its source region, *Mag. Mineral. Petrol. Sci.*, *31*, 307–317.
Shinjoe, H., Y. Orihashi, Y. Wada, T. Sumii, and S. Nakai (2007), Regional variation of whole rocl chemistry of the Miocene felsic igneous rocks in the Kii Peninsula, southwest Japan, *J. Geol. Soc. Jpn.*, *113*(7), 310–325.
Stern, R. J., M. J. Fouch, and S. Klemperer (2003), An overview of the Izu-Bonin-Mariana subduction factory, in *Inside the Subduction Factory*, vol. 138, *Monograph*, edited by J. Eiler and M. Hirschmann, pp. 175–222, AGU, Washington, D. C.
Straub, S. M. (2003), The evolution of the Izu Bonin-Mariana volcanic arcs (NW Pacific) in terms of major element chemistry, *Geochem. Geophys. Geosyst.*, *4*(2), 1018, doi:10.1029/2002GC000357.
Straub, S. M., and G. D. Layne (2003), The systematics of chlorine, fluorine, and water in Izu arc front volcanic rocks: Implications for volatile recycling in subduction zones, *Geochim. Cosmochim. Acta*, *67*, 4179–4203.
Straub, S. M., G. D. Layne, A. Schmidt, and C. H. Langmuir (2004), Volcanic glasses at the Izu arc volcanic front: New perspectives on fluid and sediment melt recycling in subduction zones, *Geochem. Geophys. Geosyst.*, *5*, Q01007, doi:10.1029/2002GC000408.
Straub, S. M., S. L. Goldstein, C. Class, A. Schmidt, and A. Gomez-Tuena (2010), Slab and mantle controls on the Sr-Nd-Pb-Hf isotope evolution of the post 42Ma Izu-Bonin Volcanic Arc, *J. Petrol.*, *51*(5), 993–1026.
Tamura, Y., et al. (2009), Silicic magmas in the Izu-Bonin oceanic arc and implications for crustal evolution, *J. Petrol.*, *50*(4), 685–723.
Tani, K., R. S. Fiske, Y. Tamura, Y. Kido, J. Naka, H. Shukuno, and R. Takeuchi (2008), Sumisu volcano, Izu-Bonin arc, Japan: Site of a silicic caldera-forming eruption from a small open-ocean island, *Bull. Volcanol.*, *70*, 547–562.
Tatsumi, Y. (2006), High-Mg andesites in the Setouchi Volcanic Belt, Southwestern Japan: Analogy to archean magmatism and continental crust formation?, *Annu. Rev. Earth. Planet. Sci.*, *34*, 467–499.
Tobin, H. J., and M. Kinoshita (2006), NanTroSEIZE: The IODP Nankai Trough Seismogenic Zone Experiment., *Sci. Drill.*, *2*, 23–27.
Todt, W., R. A. Cliff, A. Hanser, and A. W. Hofmann (1996), Evaluation of a 202Pb–205Pb double spike for high-precision lead isotope analysis., in *Earth Processes: Reading the Isotopic Code, Geophysical Monograph*, edited by A. Basu and S. Hart, pp. 429–437, AGU, Washington, D. C.
Togashi, S., T. Tanaka, T. Yoshida, K.-I. Ishikawa, A. Fujinawa, and H. Kurasawa (1992), Trace elements and Nd-Sr isotopes of island arc tholeiites from frontal arc of Northeast Japan, *Geochem. J.*, *26*, 261–277.
Underwood, M. B. (Ed.) (2007), *Sediment Inputs to Subduction Zones: Why Lithostratigraphy and Clay Mineralogy Matter*, pp. 42–85, Columbia Univ. Press, New York.

Underwood, M. B., et al. (2010), *IODP Expedition 322 Drills Two Sites to Document Inputs to The Nankai Trough Subduction Zone Sicentific Drilling, No.10*, 14–25 pp., doi:10.2204/iodp.sd.10.02.2010.

Watanabe, S., E. Widom, T. Ui, N. Miyaji, and A. M. Roberts (2006), The evolution of a chemically zoned magma chamber: The 1707 eruption of Fuji volcano, Japan, *J. Volcanol. Geotherm. Res.*, *152*, 1–19.

Yoshida, T. (2001), The evolution of Arc Magmatism in the NE Honshu Arc, Japan, *Tohoku Geophys. J.*, *36*(2), 131–149.

Zhao, X. X., H. Oda, H. C. Wu, T. Yamamoto, Y. Yamamoto, T. Nakajima, Y. Kitamura, and T. Kanamatsu (2013), Magnetostratigraphic results from sedimentary rocks of IODP's Nankai Trough Seismogenic Zone Experiment (NanTroSEIZE) Expedition 322, in *Magnetostratigraphy: Not Just a Dating Tool*, edited by L. Jovane et al., Geol. Soc. of London, U. K., doi:10.1144/SP373.14.